ARCHIVES OF ELECTRICAL ENGINEERING VOL. 64(2), pp. 291-314 (2015)

DOI 10.1515/aee-2015-0024

Dynamic response improvement of hybrid system by implementing ANN-GA for fast variation of photovoltaic irradiation and FLC for wind turbine

MAZIAR IZADBAKHSH, ALIREZA REZVANI, MAJID GANDOMKAR

Department of Electrical Engineering, Saveh Branch
Islamic Azad University, Saveh, Iran
e-mail: m.izadbakhsh@iau-saveh.ac.ir

(Received: 30.09.2014, revised: 05.02.2015)

Abstract: In this paper, dynamic response improvement of the grid connected hybrid system comprising of the wind power generation system (WPGS) and the photovoltaic (PV) are investigated under some critical circumstances. In order to maximize the output of solar arrays, a maximum power point tracking (MPPT) technique is presented. In this paper, an intelligent control technique using the artificial neural network (ANN) and the genetic algorithm (GA) are proposed to control the MPPT for a PV system under varying irradiation and temperature conditions. The ANN-GA control method is compared with the perturb and observe (P&O), the incremental conductance (IC) and the fuzzy logic methods. In other words, the data is optimized by GA and then, these optimum values are used in ANN. The results are indicated the ANN-GA is better and more reliable method in comparison with the conventional algorithms. The allocation of a pitch angle strategy based on the fuzzy logic controller (FLC) and comparison with conventional PI controller in high rated wind speed areas are carried out. Moreover, the pitch angle based on FLC with the wind speed and active power as the inputs can have faster response that lead to smoother power curves, improving the dynamic performance of the wind turbine and prevent the mechanical fatigues of the generator.

Key words: hybrid system, photovoltaic, FLC, permanent magnet synchronous generator (PMSG), ANN-GA

1. Introduction

Compared with the fossil fuels and thermal power, the renewable energy is inexhaustible and has non-pollution characteristics. Wind and PV as the types of renewable energy have received considerable attentions for producing electricity because of natural, inexhaustible resources and cost competitiveness in comparison with other types of energy. However, the hybrid energy systems are used for overcoming intermittency, uncertainty and low availability of each renewable energy source which makes the system more reliable. Hence, there have been different works concentrating on the Wind/PV hybrid system [1, 2].

There are many methods to integrate different alternative energy sources to form a hybrid system. The methods can be generally classified into two categories: DC coupling and AC coupling. The AC couple is utilized in this paper. The AC hybrid system characteristics are consisting of: 1) High reliability, if one of the energy sources is out of service, it can be isolated from the system easily, 2) Ready for the grid connection, 3) Standardizing interfacing and modular structures, 4) Easy multi-voltage and multi-terminal matching, 5) Well established scale economy.

The hybrid system is connected to the grid by using a P-Q controller of the grid side converter to exchange active and reactive power and observe system efficiency in different conditions.

PVs have high fabrication cost and low energy conversion efficiency. Therefore, using MPPT method has been recommended. In other words, the output power of a PV module varies as a function of the voltage and also, the maximum power point (MPP) is change by variation of temperature and sun irradiance [3].

In recent years, many different methods have been applied in order to reach MPP. The most prevalent technics are P&O algorithm [4, 5], IC algorithm [6, 7], fuzzy logic [8, 9] and ANN method [10-12]. According to the above mentioned researches, the benefits of the P&O and IC algorithms are: 1) low cost implementation, and 2) simple algorithm. Another drawbacks of these methods are vast fluctuations of the output power around the MPP even under a steady state which resulting in the loss of available energy [13, 14].

Using fuzzy logic can solve the two mentioned problems dramatically. In fact, with FLC, proper switching can reduce oscillations of output power around the MPP and losses. Furthermore, in this method, convergence speed is higher than the two other methods mentioned. A drawback of fuzzy logic, compared to the ANN, refers to oscillations of output power around the MPP [15, 16].

Nowadays, artificial intelligence (AI) techniques have numerous applications in determining the size of the PV systems, MPPT control and optimal structure of the PV systems. In most cases, multilayer perceptron (MLP) neural networks or radial basis function network (RBFN) have been employed for modeling PV module and MPPT controller in PV systems. ANN based controllers have been used to estimate voltages and currents corresponding to the MPP of PV module for irradiances and variable temperatures. A review on AI techniques applications in renewable energy production systems have been presented in these literatures. Neural networks are the best approximation for non-linear systems and some problems such as oscillations of output power around the MPP and time to reach the MPP are reduced [17-19]. In [10, 20-23], GA is used for data optimization and then, the optimum values are utilized for training neural networks and the results show that, the GA technic has less fluctuations in comparison with the conventional methods. However, one of the major drawbacks in mentioned papers that they are not practically connected to the grid in order to ensure the analysis of hybrid system performance, which is not considered.

In terms of WPGS is proposed as one of the outstanding renewable energy sources. Amongst the synchronous and asynchronous generators, PMSG is more favorable due to self-excitation, lower weight, smaller size, less maintenance cost and the elimination of gearbox have high efficiency and high power factor comparing to WRSG, SCIG, DFIG and so on [24].

In comparing PIDs and the fuzzy logic technics, fuzzy logic has more stability, faster and smoother response, smaller overshoot and does not need a fast processor; also it's more powerful than other non-linear controllers [25-27]. In [28-30], pitch angle based on FLC is presented. In [30] active power and in [28, 29] both reactive power and rotational rotor speed are used as input signals. As in mentioned items, wind speed's is ignored, the controller have not fast response and may cause mechanical damages to synchronous generator. Further, another problem with these studies is that they are not practically connected to the grid to analyze the system performance [29-31].

In [32], presented a power management strategy which, studied power fluctuations in a hybrid PV/wind turbine/FC power system. In [33] a simple and economic control with DC-DC converter is used for MPPT and hence maximum power extraction from the wind turbine and photovoltaic arrays. The simulation of Wind/PV hybrid system is investigated in [34]. In [35, 36], the wind-solar hybrid power system in stand-alone mode are presented.

However, all of the aforementioned papers have some drawbacks such as: 1) They are not considered FLC for controlling the output power of wind turbine and ANN-GA for MPPT in PV system to analyze and improve the dynamic performance of hybrid system, 2) In some mentioned papers, the hybrid system performance are investigated in stand-alone or not practically connected to the grid, 3) The DGs dynamic model is not included, which could have a great effect on the dynamic performances of hybrid system, 4) Some of them are not considered the detailed model in different circumstances (variation of irradiance, temperature, wind speed and load), 5) Most of them are not used the AC coupling, which is already mentioned the advantage of AC coupling comparing to DC coupling in this paper.

In this paper, the dynamic performance improvement of wind/PV hybrid system is proposed. The application of ANN-GA controller to capture the MPPT of PV panels mounted in the hybrid system. Temperature and irradiance as inputs data are given to GA and the optimal voltages (V_{mpp}) corresponding to the MPP are obtained; then, these optimum values are used in neural network training. As well as, the FLC is used to control the output power of the grid connected wind turbine in high speeds with comparing to PI controller.

2. Photovoltaic cell model

Figure 1 shows the equivalent circuit of one PV cell [5]. Characteristic of one solar array is explained by following Equations.

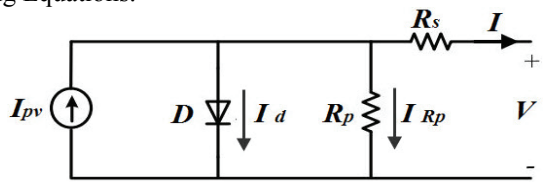

Fig. 1. Equivalent circuit of one PV array

$$I_{PV} = I_d + I_{RP} + I, \tag{1}$$

$$I = I_{pv} - I_0\left[\exp\left(\frac{V + R_S I}{V_{th} n}\right) - 1\right] - \frac{V + R_S I}{R_p}. \tag{2}$$

Where, I is the output current, V is the output voltage, I_{pv} is the generated current under a given insolation, I_d is diode current, I_{RP} is the shunt leakage current, I_0 is the diode reverse saturation current, n is the ideality factor for a p-n junction, R_s is the series loss resistance, and R_P is the shunt loss resistance. V_{th} is known as the thermal voltage. Red sun 90 W is taken as the reference module for simulation and the name-plate details are given in Table 1. The array is the combination of 6 cells in series and 6 cells in parallel of the 90 W module; hence an array generates 3.2 kW.

Table 1. Red Sun 90 W

I_{MP} (current at maximum power)	4.94 A
V_{MP} (voltage at maximum power)	18.65 V
P_{MAX} (maximum power)	90 W
V_{OC} (open circuit voltage)	22.32 V
I_{SC} (short circuit current)	5.24 A
N_P (total number of parallel cells)	1
N_S (total number of series cells)	36

3. Maximum Power tracking – neural network and GA technic

3.1. The Steps of Implementing GA and ANN

In order to pursue the optimum point for maximum power in any environmental conditions, ANN and GA technic are implemented. Besides, GA is used for optimum values and then, optimum values are used for training ANN [10, 22]. The procedure employed for implementing GA is as follows [23, 37]: 1) Defining the objective function and recognizing the design parameters, 2) Defining the initial production population, 3) Evaluating the population using the objective function, 4) Conducting convergence test stop, if convergence is provided. The objective function of GA is used for its optimization (using Matlab software) by the following: finding the optimum $X = (X_1, X_2, X_3,..., X_n)$ to put the $F(X)$ in the maximum value, where the number of design variables are considered as 1. X is the design variable equal to array current and also, $F(X)$ is the array output power which should be maximized [22, 23]. To determine the objective function, the power should be arranged based on the current of array (I_X). The GA parameters are given in Table 2.

$$F_{(x)} = V_X * I_X, \tag{3}$$

$$0 < I_X < I_{SC}. \tag{4}$$

Table 2. The GA parameters

Number of design variable	1
Population size	25
Crossover constant	75%
Mutation rate	15%
Maximum Generations	30

The current constraint should be considered too. By maximizing this function, the optimum values for V_{mpp} and MPP will result in any particular temperature and irradiance intensity.

3.2. MPPT Improvement by Combination of Proposed ANN with GA

Neural networks are most appropriate for the approximation (modeling) of nonlinear systems. Non-linear systems can be approximated by multi-layer neural networks and these multi-layer networks have better result in comparison with the other algorithm [16, 18]. In this paper, feed forward neural network for MPPT process control is used. The important section of this technic is that, the required data for training process must be obtained for each PV module and each specific location [11]. Based on the PV characteristic which depend on PV model and climate change, neural network should be trained periodically. Neural network inputs can be selected as PV array parameters like V_{oc}, I_{sc} and climate data, temperature or both of them. The output is usually one reference signal like duty cycle or DC link voltage or V_{mpp}.

The proposed neural network has three layers which the temperature and solar irradiance as input variables and output variable of the neural network is V_{mpp} corresponding to MPP as shown in Figure 2. Also, a simple block diagram of the PV system with the proposed MPPT is shown in the Figure 3.

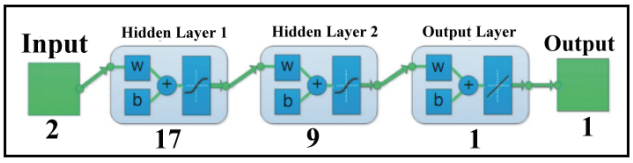

Fig. 2. Feed forward neural network for MPPT

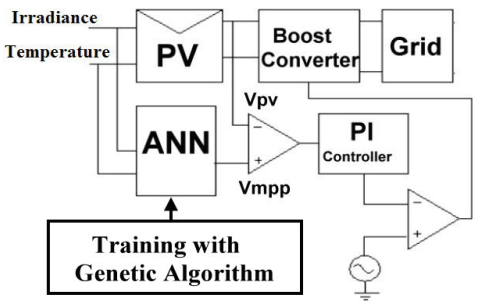

Fig. 3. Proposed MPPT scheme

The output characteristic of arrays has changed during time and environmental conditions. Therefore, needing for periodic training of the neural network in order to increase precision is essential. According to Figure 4 for training of the neural network a set of 390 data is used (temperatures between –5°C to 55°C and irradiance between 0.05 to 1 kilo-watt per square meters (kW/m^2)) and also, a set of 390 V_{mpp} corresponding to MPP is achieved by GA that is shown in Figure 5. Our aim is to show the effectiveness of the proposed method in comparing to conventional methods by using Matlab software. However, in the real conditions it should consider all level of the temperature.

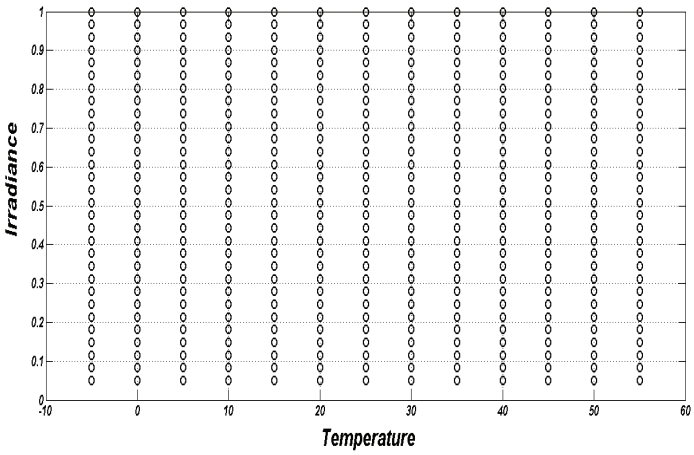

Fig. 4. Inputs data of irradiance and temperature

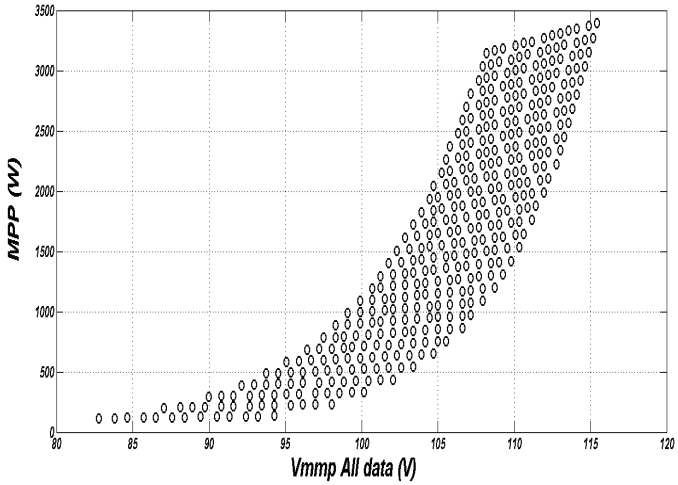

Fig. 5. The output of V_{mpp}-MPP optimized by GA

In order to implementation of the ANN for MPPT, first it should be determined the number of layers, number of neurons in each layer, transmission function in each layer and type of training network. The proposed ANN in this paper has three layers which first and second

layers have respectively 17 and 9 neurons and third layer has 1 neuron. The transfer functions for first and second layers are Tansig and for third layer is Purelin. The training function is Trainlm. The acceptable sum of squares for network is supposed to be 10^{-9}. Which training this neural network in 900 iterations, will converge to a desired target. After training, the output

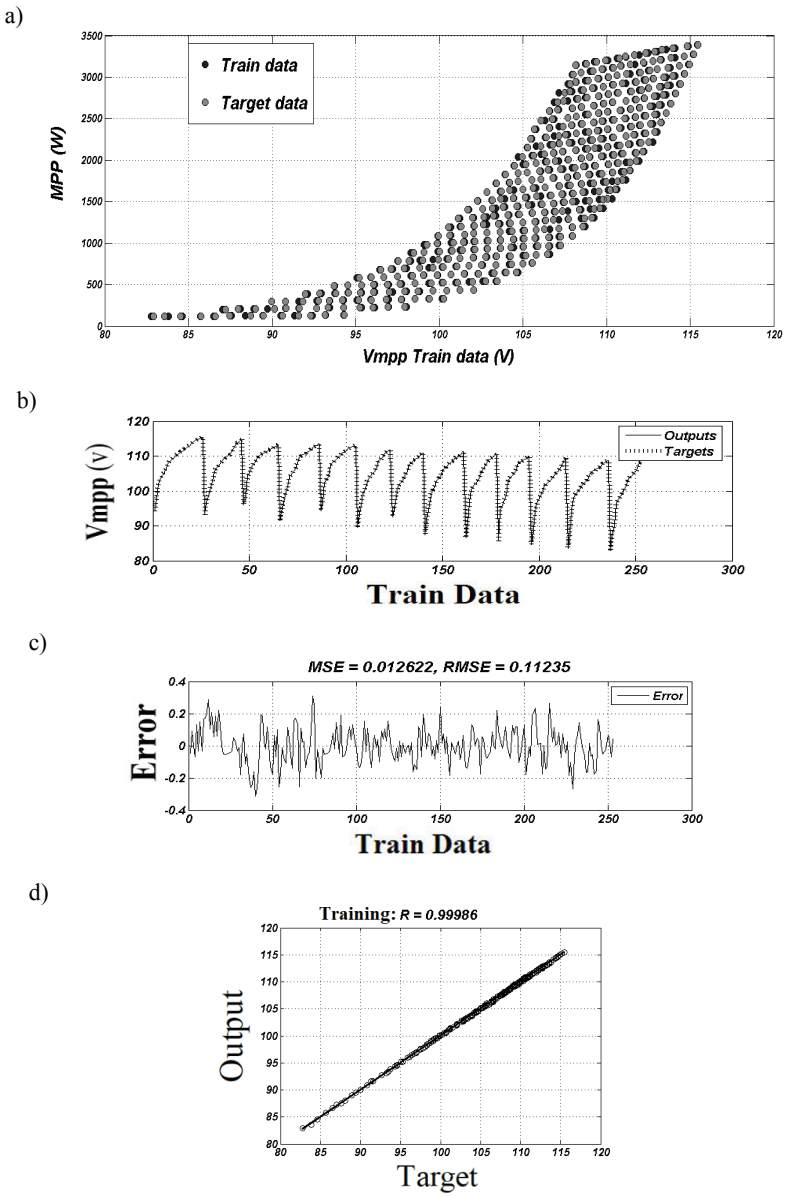

Fig. 6. Shown the output of the neural network by fallowing: a) The output of the neural network with the amount of target data; b) The output of the neural network V_{mpp} with the amount of target data; c) Percentage of the total error of the V_{mpp} training data; d) Train output versus target

a)

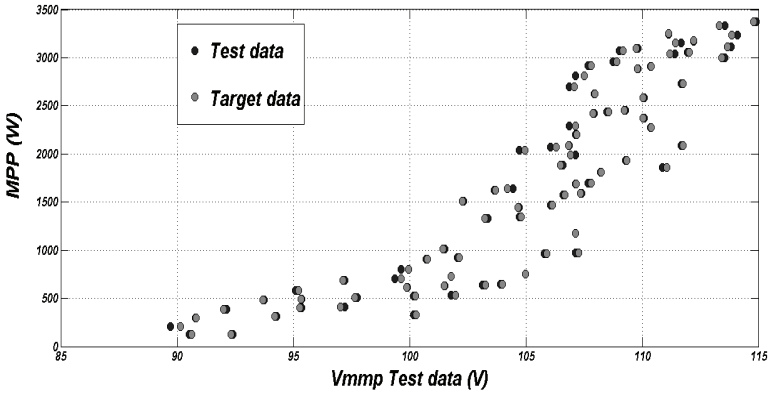

b)

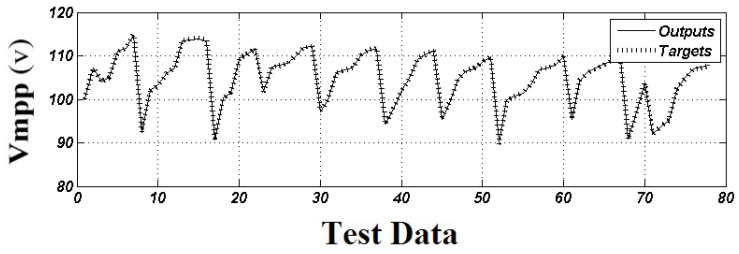

c)

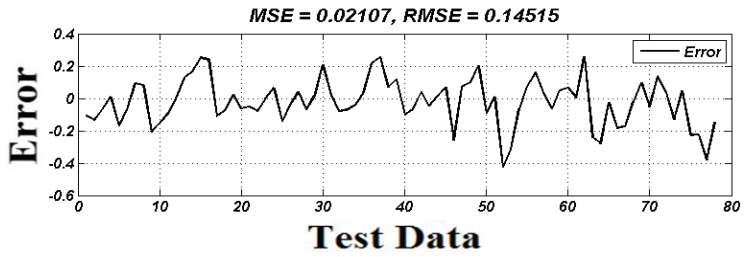

d)

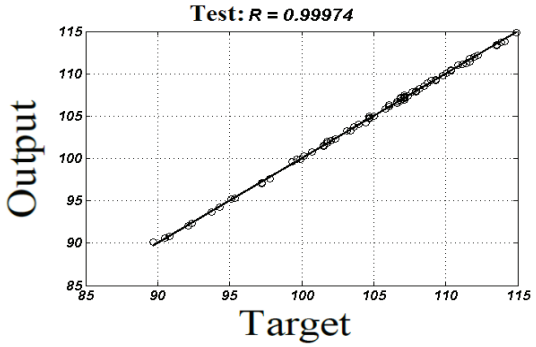

Fig. 7. Shown the output of the neural network test by following: (a) The output of the neural network test with the amount of target data; (b) The output of the neural network test V_{mpp} with the amount of target data; (c) Percentage of the total error of the V_{mpp} test data; (d) Test output versus target

of training network should be close to optimized output from GA. Figure 6 show the output of the neural network with the amount of target. A set of 80 data is used for the ANN test. Figure 7 illustrate the output of the neural network test with the amount of target which showing a negligible training error percentage of about 0.2%.

4. WPGS configuration

The diagram of a WPGS based on the PMSG is illustrated in Figure 8. Turbine output is rectified by using the uncontrolled rectifier. Then DC link voltage is adjusted by PI controller until it reached a constant value and then, this constant voltage is inverted to AC voltage using sinusoidal pulse width module (PWM) inverter. Inverter adjusted the DC link voltage and injected active power by d-axis and injected reactive power by q-axis using P-Q control method. Furthermore, turbine output is regulated by pitch angle based on FLC in extra high wind speeds.

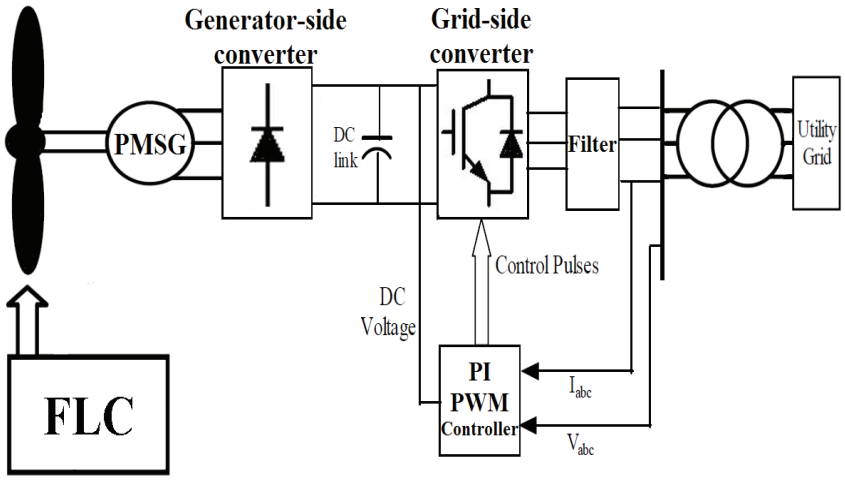

Fig. 8. The block diagram of WPGS

4.1. Wind turbine modeling

The amount of electricity a turbine is able to produce depends on the speed of the rotor and the speed of the wind that propels the rotor [31, 38]. Aerodynamic wind power is calculated in following equations.

$$P = 0.5\rho A C_p(\lambda,\beta) V_w^3, \tag{5}$$

$$\lambda - \frac{W_m R}{V_w}, \tag{6}$$

$$C_p(\lambda,\beta)=0.5176\left(\frac{116}{\lambda_i}-0.4\beta-5\right)e^{\frac{-21}{\lambda_i}}, \tag{7}$$

$$\lambda_i=\left[\frac{1}{\lambda+0.08\beta}-\frac{0.035}{\beta^3+1}\right]^{-1}. \tag{8}$$

Where P, ρ, A, V_w, W_m and R are power, air density, rotor swept area of the wind turbine, wind speed in m/sec, rotor speed in rad/s and radius of turbine respectively. Also, C_p is the aerodynamic efficiency of rotor [39]. Furthermore, C_P is depends on tip speed ratio (TSR) and blade pitch angle. Figure 9 illustrates the typical variation of C_P respect to the TSR for various values of the pitch angle (β).

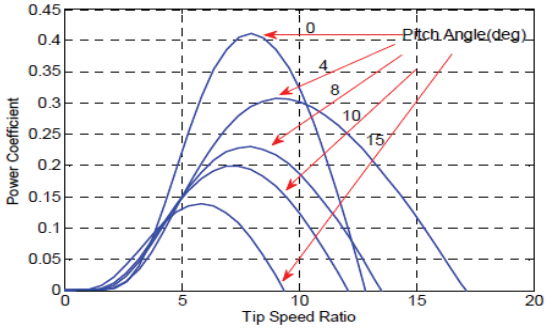

Fig. 9. C_P vs. λ (TSR) for various pitch angles β

4.2. PMSG modeling

A synchronous generator with reference to Park's transformation is illustrated which d-axis is rotating along magnetic field direction. PMSG voltage equations are given by [38]:

$$\frac{di_{ds}}{dt}=\frac{1}{L_d}\left[-V_{ds}-R_s i_{ds}+\omega L_q i_{qs}\right], \tag{9}$$

$$\frac{di_{qs}}{dt}=\frac{1}{L_q}\left[-V_{qs}-R_s i_{qs}-\omega L_d i_{ds}+\omega\phi_m\right]. \tag{10}$$

Where V_{ds}, V_{qs} are q and d axis machine voltages, I_{ds}, I_{qs} are q and d axis machine currents, R_s: Stator Resistance, W: electrical angular frequency, L_d: d-axis inductance, L_q: q-axis inductance, ϕ_m: amplitude of the flux linkage caused by permanent magnet. If rotor is cylindrical ($L_d \approx L_q = L_s$), the electromagnetic torque (EM) equation written as following:

$$T_e=\frac{3}{2}p\phi_m i_{qs}, \tag{11}$$

where p is the number of pole pairs of the PMSG.

4.3. Pitch angle based on FLC

FLC is made of three parts which is demonstrated in Figure 10. First part is fuzzification which is the process of changing a real scalar value into a fuzzy set. Second part is fuzzy inference system that combines IF-THEN statements based on fuzzy principle and finally, it has defuzzification which is the process that changes a fuzzy set into a real value in output [29].

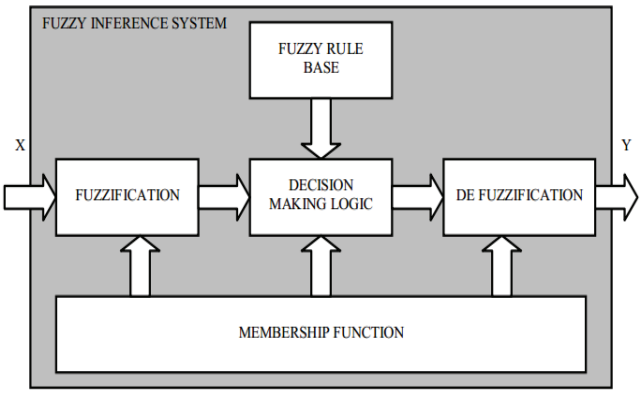

Fig. 10. The structure of fuzzy logic system

The presented FLC consists of two input signals and one output signal. The first input signal is based on the deviation between active power and the rated value in P.U, which is mentioned as error signal. Thus, its positive value indicates turbine's normal operation and its negative value shows the extra power generation during the above rated wind speed. In this case, controller should modify pitch angle degree by increasing the nominal value. The pitch angle degree is regulated on zero in a normal condition. The whole wind energy can be converted to mechanical energy and when the pitch angle starts to increase from the zero value, the wind attach angle to the blades will be increased, thereby leading to aerodynamic power reduction and consequently, drawing down the output power. Besides, the second signal is taken from anemometer Nacelle [39].

Controller's response is so faster when wind speed is used as an input signal compared to the time when inputs are rotor rotational speed or active power in large turbines with a high moment of inertia [28-30]. However, mechanical erosion in large and high speed turbines is diminished by adjusting this FLC. Designing a pitch angle based on FLC for wind turbine power adjustment in high wind speeds is being proposed in this paper. Three Trapezoidal membership functions are considered in this paper. Furthermore, Min-Max method is used as a defuzzification reference mechanism for centroid. Given membership functions are shown in Figure 11.

Moreover, the rules implemented to obtain the required pitch angle (β) are shown in Table 3. The linguistic variables are represented by VG (very great), SG (small great), OP (optimum), SL (small low), and VL (very low) for error signal and VL (very low), SL (small low), OP (optimum), SH (small high) and VH (very high) for wind speed signal and NL (nega-

a)

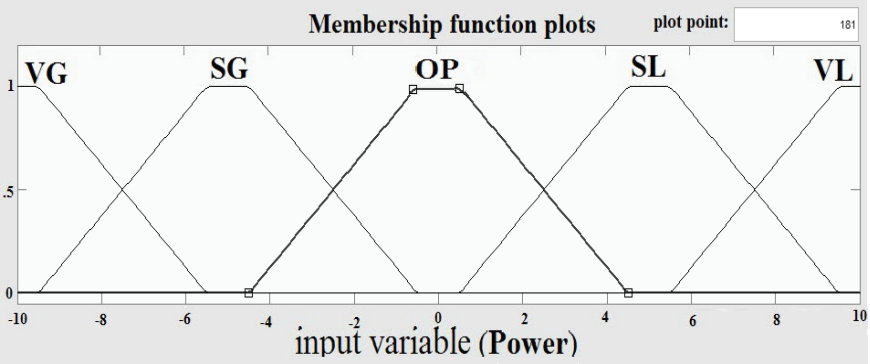

b)

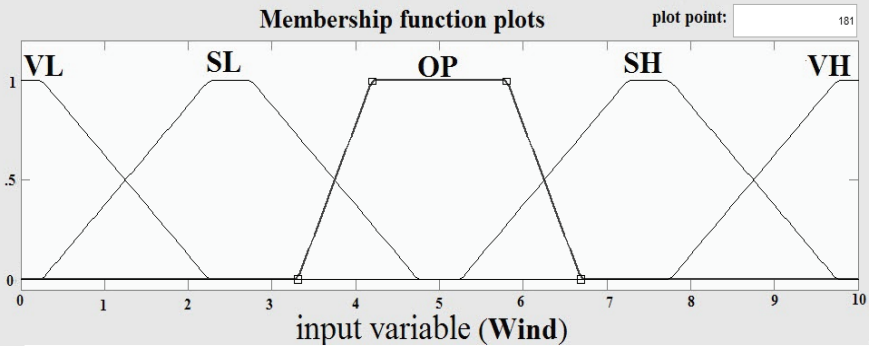

c)

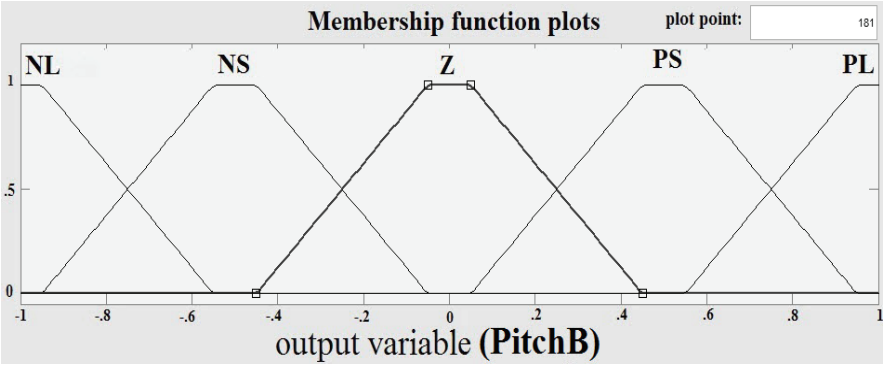

Fig. 11. The membership function of fuzzy logic: (a) Membership functions of active power (error signal); (b) Membership functions of wind speed; (c) Membership functions of output (β)

tive large), NS (negative small), Z (zero), PS (positive small) and PL (positive large) for output signal, respectively. The three dimensional curve in FLC is shown in Figure 12.

Table 3. Fuzzy rules

Pitch command		**Active power (error)**				
Wind speed		VG	SG	OP	SL	VL
	VL	PL	PS	Z	Z	Z
	SL	PL	PS	Z	Z	Z
	OP	PL	PS	Z	Z	Z
	SH	PL	PS	PS	PS	PS
	VH	PL	PL	PL	PL	PL

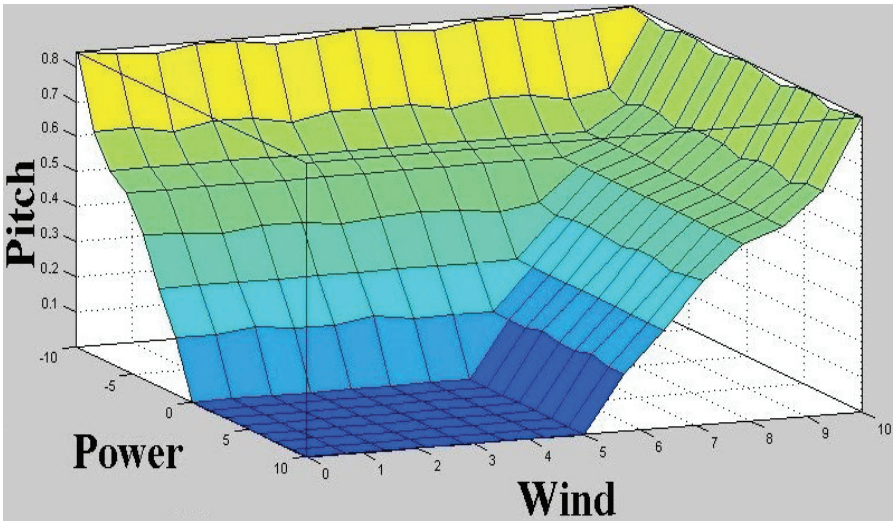

Fig. 12. The three dimensional curve in FLC

5. P-Q control strategy

The inverter by PWM technic produces high frequency harmonics, that need to utilize filter to eliminate them and the voltage source inverter (VSI) can play role as an ideal sinusoidal voltage source.

Since wind power is fluctuates due to wind velocity, output voltage and frequency change continuously. A bridge rectifier provides AC to DC and then, DC link voltage using PI controller to obtain constant value, then DC voltage will be inverted to get desired AC voltage.

$$P = \frac{3}{2}\left(V_{gd} I_d + V_{gq} I_q\right), \tag{12}$$

$$Q = \frac{3}{2}\left(V_{gq} I_d + V_{gd} I_q\right), \tag{13}$$

If synchronous frame is synchronized with the grid voltage, voltage vector is $V = V_{gd} + j0$ which, active and reactive power may be as following:

$$P = \frac{3}{2} V_{gd} I_d , \tag{14}$$

$$Q = \frac{3}{2} V_{gq} I_d , \tag{15}$$

Synchronous reference is calculate quantities of d-axis, q-axis and zero sequence in two axis rotational reference vector for three phase sinusoidal signal illustrated in Figure 13. The equations are given by (16), (17).

$$\begin{bmatrix} V_d \\ V_q \\ V_0 \end{bmatrix} = C \begin{bmatrix} V_a \\ V_b \\ V_c \end{bmatrix}, \quad \begin{bmatrix} i_d \\ i_q \\ i_0 \end{bmatrix} = C \begin{bmatrix} i_a \\ i_b \\ i_c \end{bmatrix}, \tag{16}$$

$$C_{dq0} = \frac{2}{3} \begin{bmatrix} \cos\theta & \cos(\theta - \frac{2\pi}{3}) & \cos(\theta + \frac{2\pi}{3}) \\ -\sin\theta & -\sin(\theta - \frac{2\pi}{3}) & -\sin(\theta + \frac{2\pi}{3}) \\ \frac{1}{2} & \frac{1}{2} & \frac{1}{2} \end{bmatrix} \tag{17}$$

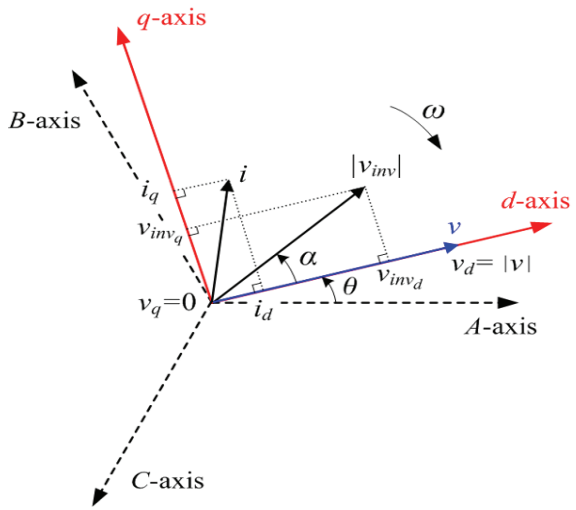

Fig. 13. The synchronous reference machine

Inverter control model is depicted in Figure 14. The goal of controlling the grid side is keeping the DC link voltage in a constant value regardless of production power magnitude.

Inverter control strategy is consisting of two control loops. Internal control loop is control the grid current and external control loop is control the voltage .Internal control loop which is responsible for power quality such as low total harmonic distortion (THD) and improvement of power quality and external control loop is responsible for balancing the power. In grid-connected mode hybrid system must supply local loads to decrease power from the main grid. One of the main aspects of P-Q control loop is operating in grid connected and stand-alone mode. The advantages of this operation mode are higher power reliability and higher power quality [40]. Active and reactive components of the injected current are i_d and i_q, respectively. For the independent control of both id and i_q, the decoupling terms are used. To synchronize the converter with grid, a three phase lock loop (PLL) is used. PLL reduces the difference between grid phase angle and the inverter phase angle to zero using PI controller, thereby synchronizing the line side inverter with the grid [41].

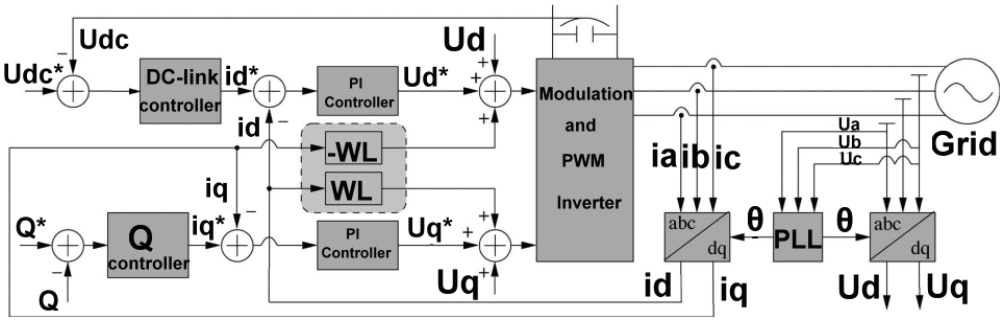

Fig. 14. Control scheme for inverter

6. Simulation results

In this section, simulation results under different terms of operation in hybrid system are presented. The block diagram of hybrid system is shown in Figure 15a). Our target is to show the effectiveness of the proposed methods (ANN-GA and FLC) with conventional methods in PV and WPGS and enhanced the dynamic performance of hybrid system to meet the load demand in different conditions (Load, wind speed, irradiance and temperature variations) by using AI techniques. The important priority of this hybrid system is supplying the 100 kW AC load (electrical load) requirement in critical circumstances. Structure of the P/Q controller is depicted in Figure 15b). The grid voltage and frequency are 220 V and 60 Hz respectively. The PV and wind systems connected to the grid by applying P-Q controller are shown in Figures 16 and 17, respectively. Detailed model descriptions are given in Appendix A.

6.1. Case 1: Variation of irradiance and temperature

The main objective of this case is investigated comparative study of four widely-adopted MPPT algorithms under variations of irradiance and temperature in PV system. The hybrid

system is connected to the main grid that includes 3.2 kW photovoltaic system, 97 kW wind turbine system and the amount of load is 100 kW. There is no power exchange between hybrid system and grid in normal condition.

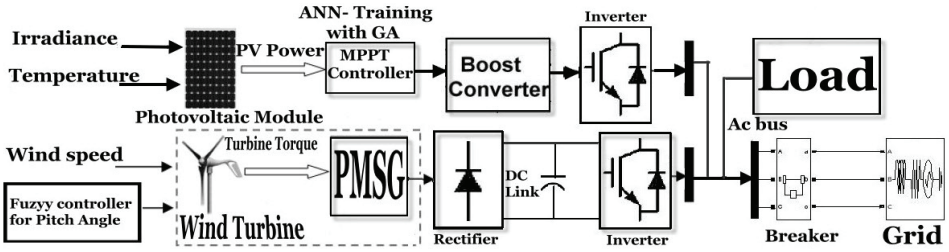

Fig. 15a. Block diagram of proposed wind/PV hybrid system

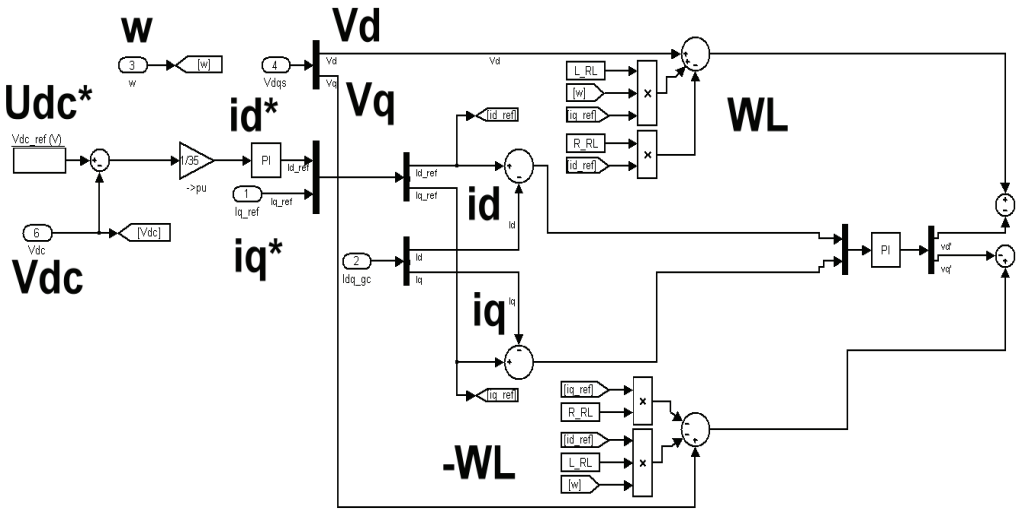

Fig. 15b. Structure of the P-Q controller

The following simulation is presented for different insolation levels at fixed temperature of 25°C as shown in Figure 18a). The output voltage and the current of PV are depicted in Figures 18b) and 18c), respectively. When irradiance is increased at $t = 4$ s and $t = 8$ s, it lead to increase in the output current of PV as shown in Figure 18c). The evaluation of the proposed controller is compared and analyzed with the conventional techniques of fuzzy logic, P&O and IC. The proposed MPPT algorithm can track accurately the MPP when the irradiance changes continuously; also, it produces extra power rather than aforementioned methods as indicated in Figure 18d). Therefore, the injected power from the main grid to hybrid system is decreased as demonstrated in Figure 18e).

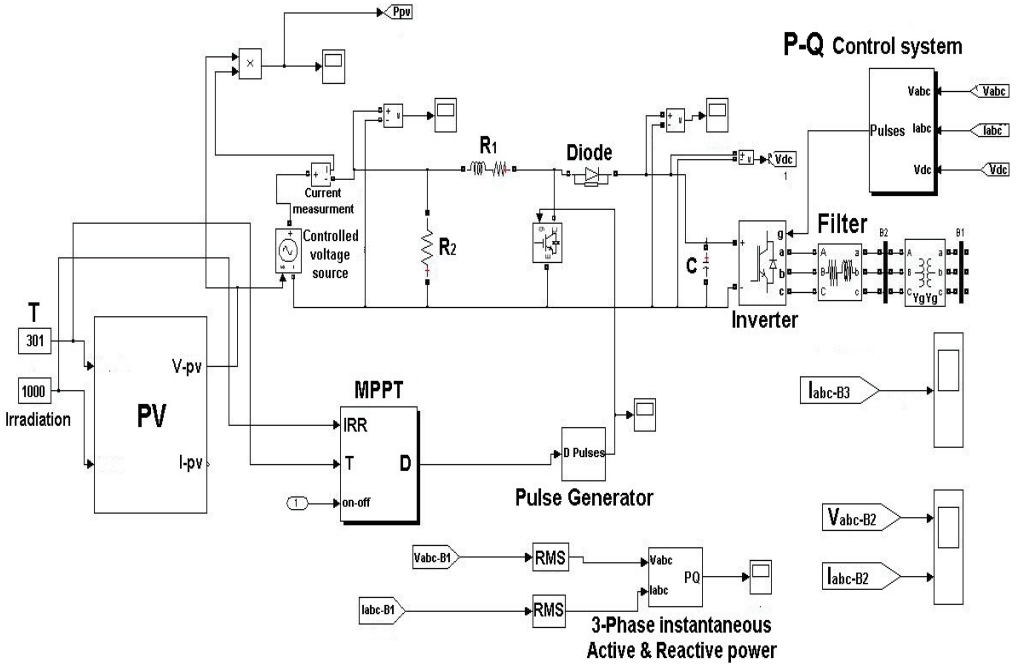

Fig. 16. PV system in grid-connected mode by applying P-Q controller

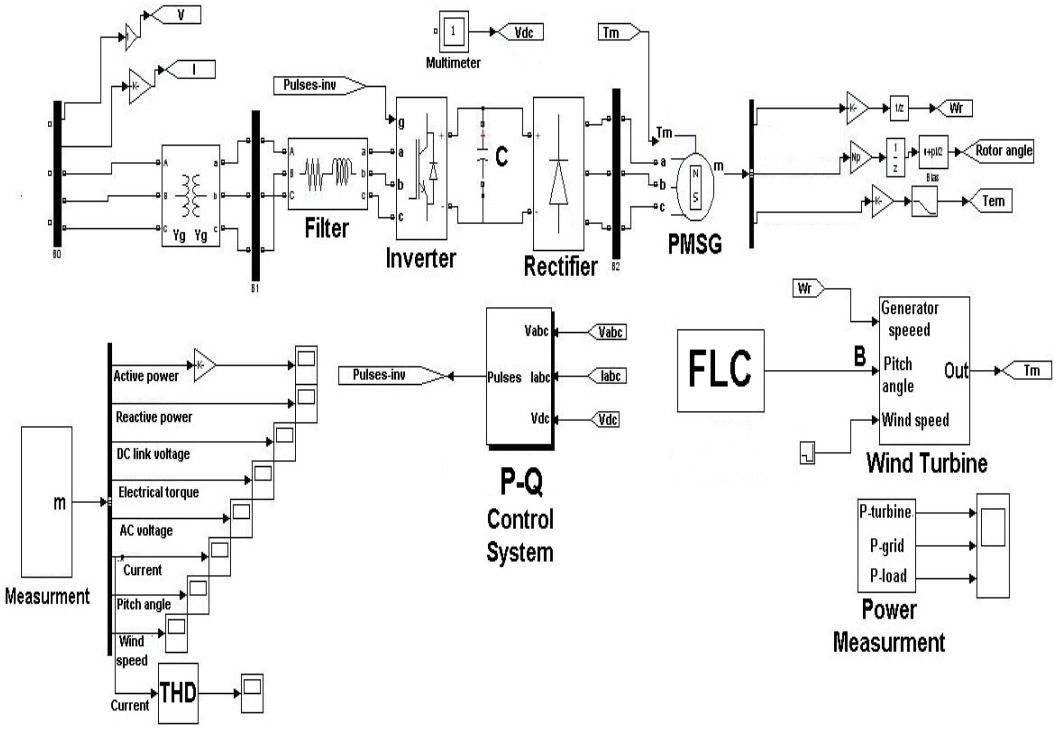

Fig. 17. WPGS in grid-connected mode by applying P-Q controller

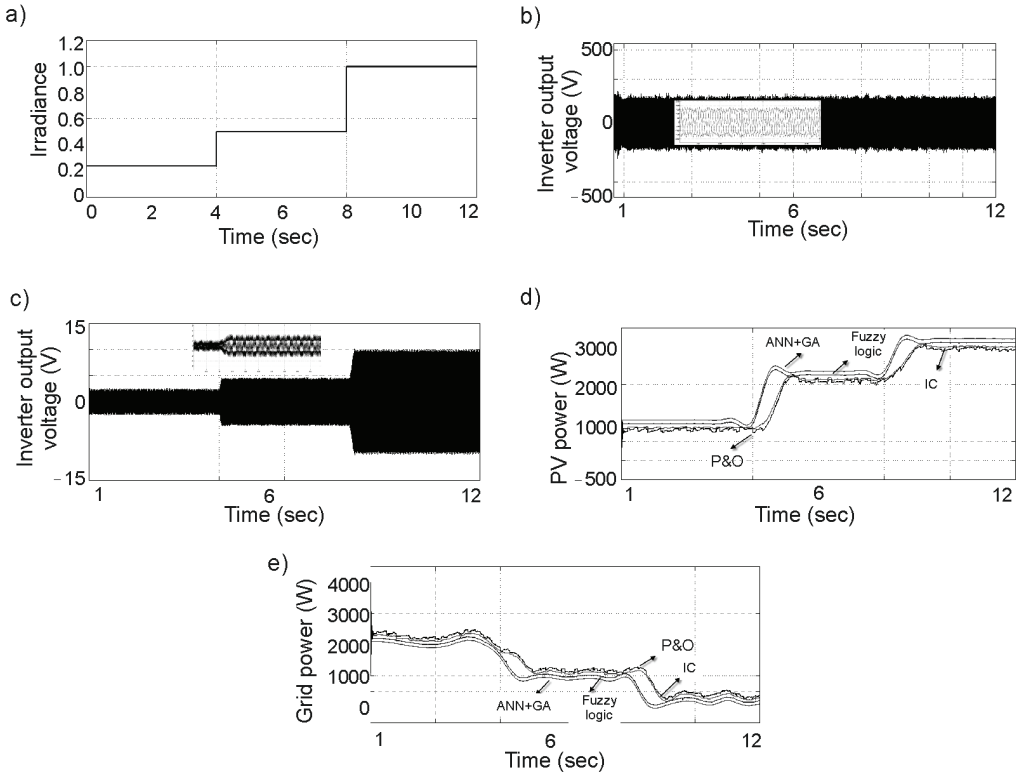

Fig. 18. Simulated results for PV (Variation of Irradiance) in case 1: a) Irradiance; b) Inverter output voltage; c) Inverter output current; d) PV power; e) Grid power

Table 4 shows the comparison of real power value and presented methods in the different irradiation conditions. In order to realize a precise analysis of the ANN-GA technique, different temperature levels at fixed insolation of 1000 W/m^2 as shown in Figure 19a) is considered. The grid voltage is indicated in Figure 19b). The ANN-GA method shows smother power, less oscillating and better stable operating point than P&O, IC and fuzzy logic. It has more accuracy for operating at MPP and also, it generates exceeding power rather than mentioned techniques as depicted in Figure 19c). Consequently, the grid power injection to hybrid system is declined as illustrated in Figure 19d). Table 5 shows the comparison of real power value and presented methods in the different temperature conditions.

Table 4. Output power values of solar array (watt) in various irradiation conditions

Irradiance variations	**PV power**				
	Real value	ANN+GA	Fuzzy logic	IC	P&O
0s to 4s	1020	1007	1000	891	886
4s to 8s	2430	2421	2413	2252	2220
8s to 12s	3200	3191	3181	2985	2970

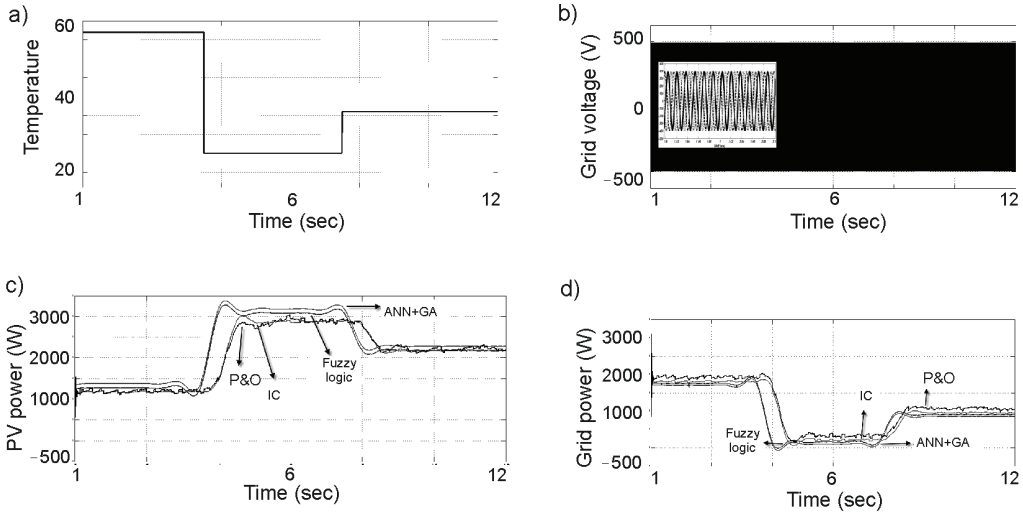

Fig. 19. Simulated results for PV (Variation of Temperature) in case 1: a) Temperature; b) Grid voltage; c) PV power; d) Grid power

Table 5. Output power values of solar array (watt) in various temperature conditions

Temperature variations	PV power				
	Real value	ANN+GA	Fuzzy logic	IC	P&O
0s to 3.5s	1435	1427	1416	1387	1381
3.5s to 7.5s	3200	3191	3179	2981	2974
7.5s to 12s	2352	2341	2303	2298	2295

6.2. Case 2: variation of wind speed and load

In this case, the evaluation of FLC with comparing to conventional PI controller in pitch angle of wind system is carried out. The variations of wind speed and load to analyze of hybrid system performance are implemented. There is no power exchange between hybrid system and grid in normal condition. During $0 < t < 1$ s, the load power is 100 kW and at $t = 1$ s, it has 50% step increase in load that is constant until $t = 2$ s. Then, at $t = 3$ s, it has step decrease 35% in load power, that is constant until t = 3.5 s.

Wind speed during $0 < t < 4.5$ s, is 12 m/s which at $t = 4.5$ s, it is reduced to 9.5 m/s. Then, during $1 < t < 1.5$ s, wind speed is 10 m/s and after that, at $t = 6.5$ s, it is extremely increased to 18 m/s. By designing FLC, when wind speed is more than nominal speed (12 m/s), turbine output power is increased by extremely increasing wind speed; however, with PI controller, the power is constant at a high level power and in the presence of FLC, it is more reduced to the nominal power and made it more smoother, thereby leading to improvement of dynamic performance and the prevention of mechanical fatigue to PMSG.

Figure 20a) shows the variation of wind speed. The reactive power produced by the wind turbine is regulated at zero such that the power factor maintained unity as shown in Figure 20b). One of the most important aspects of using DG sources and connecting them to grid is

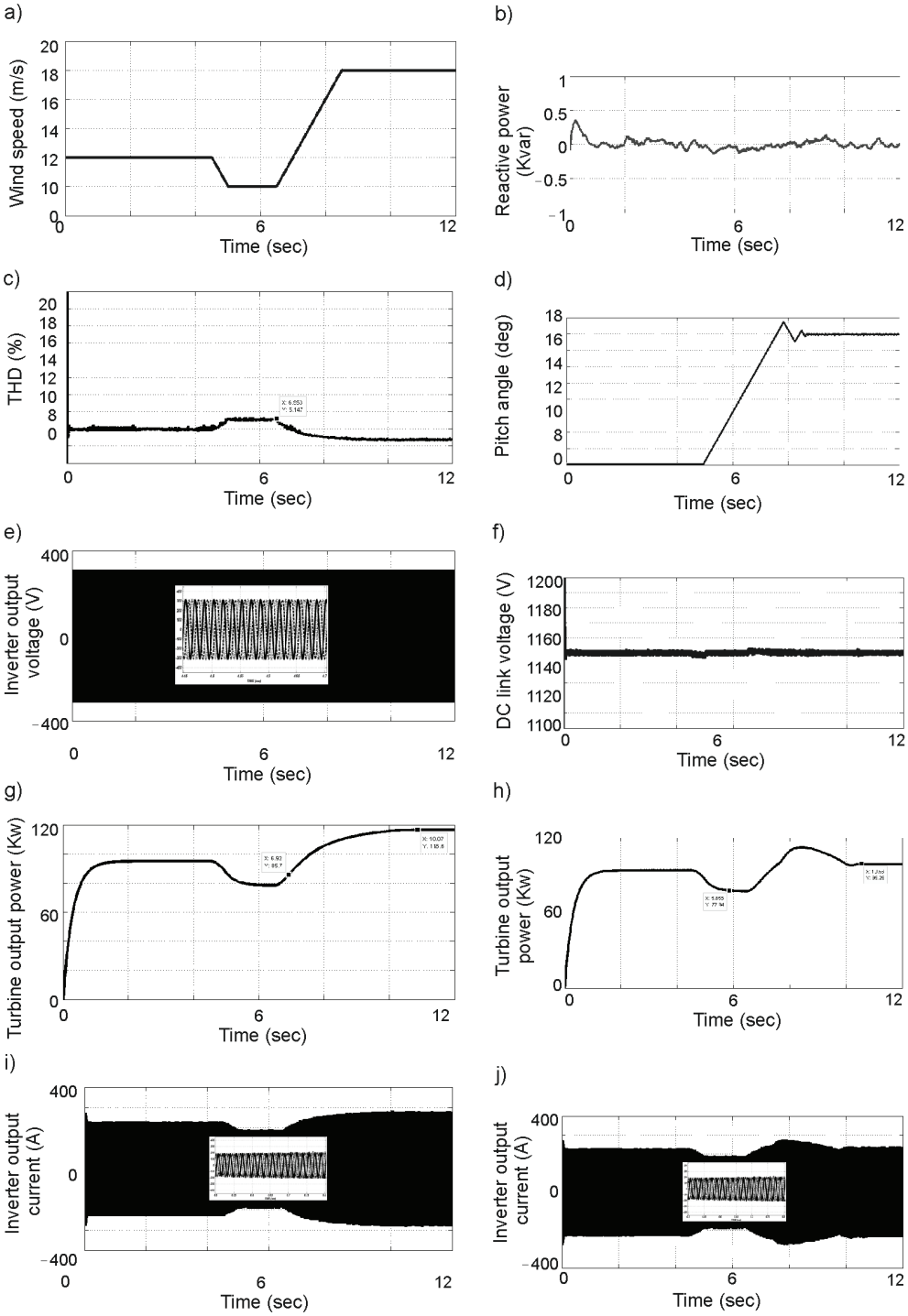

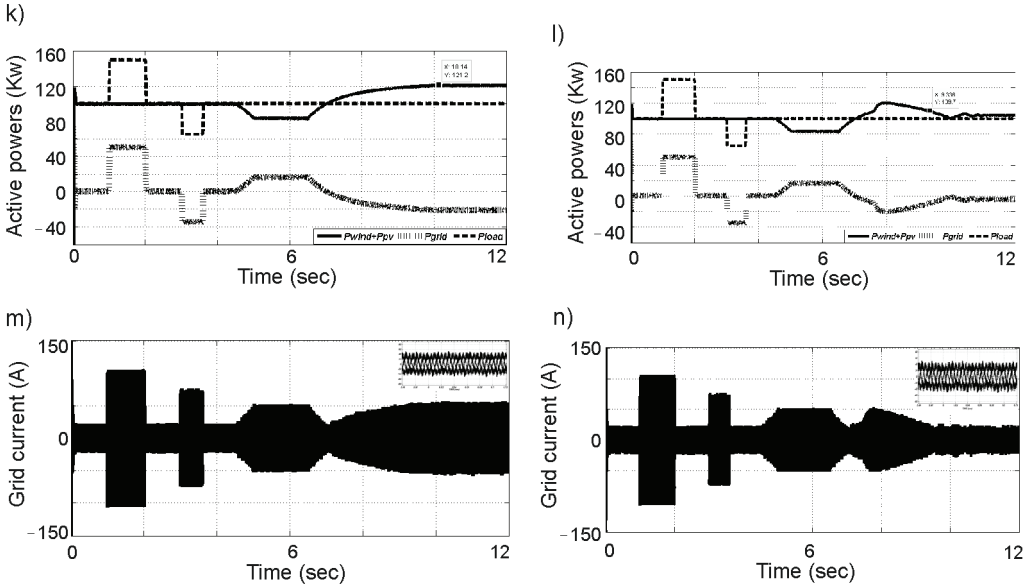

Fig. 20. Simulated results for WPGS in case 2: a) Wind speed; b) Reactive power; c) THD (%); d) Variation of pitch angle by FLC; e) Inverter output voltage; f) DC link voltage; g) Inverter output current with absence of FLC; h) Inverter output current with presence of FLC; i) Turbine output power with absence of FLC; j) Turbine output power with presence of FLC; k) Active powers with absence of FLC; l) Active powers with presence of FLC; m) Grid current with absence of FLC; n) Grid current with presence of FLC

keeping the THD at the minimum of its value. According to IEEE Std.1547.2003, it should be around 5%. In THD curve, it is around 4% to 6%. THD is shown Figure 20c). Figure 20d) displays the variation of pitch angle in the presence of FLC. As can be seen, in normal situations, the pitch angle is set as zero. Inverter output voltage is invariant, which is shown in Figure 20e). DC link voltage remains at a constant value (1150 V), thereby proving the effectiveness of the established FLC as illustrated in Figure 20f). At wind speeds above the rated wind, the extracted wind power has to be limited by increasing the pitch angle (β). Figures 20g) and 20h) show the turbine output power in the absence and presence of FLC according to wind speed. It is obvious that FLC make a smoother power curve. Table 6 shows the comparison of real power value and proposed methods in the different wind speed conditions, which it shows in high wind speeds, the output power of WPGS by using FLC method is more declined and more prevent the mechanical fatigues to PMSG. Figures 20i) and 20j) show inverter output current in the absence and presence of FLC, respectively. It shows the effectiveness of FLC by increasing pitch angle degree. The exceeding power of wind turbine is limited and also, the inverter output current is reduced in comparison with PI controller. Pitch angle based on FLC is more limited the exceeding output power of turbine. Therefore, by the reduction of injected output power of wind turbine, the injection of extra total active power of hybrid system to grid is more declined which is illustrated in Figures 20k) and 20l). In Figures 20k) and 20l), the effectiveness of FLC is evaluated. Figures 20m) and 20n) show the grid current in the absence and presence of FLC, respectively.

Table 6: Output power values of WPGS (kW) in various Wind speeds

Wind speed variations	Wind power		
	Real value	PI	FLC
0 s to 4.5 s	97.1	97.1	97.1
4.5 s to 6.5 s	77.5	77.5	77.5
6.5 s to 12 s	124.860	118.600	99.290

7. Conclusion

In this paper, the dynamic response of the grid connected Wind/PV hybrid system under load circumstances and the variations of wind speed, irradiance and temperature were proposed. The control strategy modeling of a DC/AC grid connected converter was presented. Inverter adjusted the DC link voltage and active power was fed by d-axis and reactive power was fed by q-axis (using P-Q control mode).

The simulation results indicated that using the ANN-GA controller could dramatically reduce the disadvantages of previous approaches. In fact, ANN-GA controller could decrease oscillations of output power around the MPP and increase convergence speed to achieve the MPP in comparison with conventional methods in the grid-connected mode. Also, the proposed FLC in the pitch angle, by adding wind speed as an input signal, could have faster and smoother response. The advantage of FLC was that it kept the turbine output in an admissible value and could prevent more mechanical fatigue and also, the dynamic performance of wind turbine could be improved. In other words, by increasing the pitch angle via FLC, the exceeding power of the wind turbine was limited, reaching the nominal value and reducing the inverter output current. Therefore, by the reduction of injected the output power of the wind turbine, the injection of extra total active power of the hybrid system to the grid was decreased. It was clear that, the Wind/PV hybrid system by applying FLC in pitch angle with the cooperation of grid could easily meet the load demand.

Appendix A: Description of the Detailed Model

PV parameters: output power = 3.2 kW, Carrier frequency in V_{MPPT} PWM generator: 4.3 kHz and in grid-Sid controller: 5 kHz, boost converter parameters: $L = 3.5$ mH, $C = 630$ μF, PI coefficients in grid-side controller: $K_{pVdc} = 3.5$, $K_{iVdc} = 7.3$, $K_{pId} = 8.4$, $K_{iId} = 343$, $K_{pIq} = 8.4$, $K_{iIq} = 343$.

PMSG parameters: output power = 97 kW, Stator resistance per phase = 2.8 Ω, inertia = $0.8e^{-3}$ kg-m^2, torque constant 12N-M/A, Pole pairs = 8, Nominal speed = 12 m/s, $L_d = L_a =$ 7.3 mH.

Grid parameters: X/R = 7, and other parameters, DC link capacitor = 5600 μF, DC link voltage = 1150 V. PI coefficients in grid-side controller: $K_{pVdc} = 9$, $K_{iVdc} = 473$, $K_{pId} = 0.94$, $K_{iId} = 8$, $K_{pIq} = 0.94$, $K_{iIq} = 8$.

References

[1] Rezvani A., Gandomkar M., Izadbakhsh M., Ahmadi A., *Environmental/economic scheduling of a micro-grid with renewable energy resources.* Journal of Cleaner Production 87: 216-226 (2015).

[2] Izadbakhsh M., Gandomkar M., Rezvani A., Ahmadi A., *Short-term resource scheduling of a renewable energy based micro grid.* Renewable Energy 75: 598-606 (2015).

[3] Farret F.A., Simões M.G., *Integration of Alternative Sources of Energy*, New York, NY, USA, Wiley (2006).

[4] Hayrettin C., *Model of a photovoltaic panel emulator in MATLAB-Simulink.* Turk Turkish Journal of Electrical Engineering & Computer Sciences 21: 301-308 (2013).

[5] Villalva M.G., Gazoli J.R., Filho E., *Comprehensive Approach to Modeling and Simulation of Photovoltaic Arrays.* IEEE Transactions on Power Electronics 24(5): 1198-1208 (2009).

[6] Chu C.C., Chen C.L., *Robust maximum power point tracking method for photovoltaic cells: a sliding mode control approach*, Solar Energy 83(8): 1370-1378 (2009).

[7] Liu F.F., Duan S., Liu B., Kang Y., *A variable step size INC MPPT method for PV systems,* IEEE Transaction on Industrial Electronics 55(7): 622-2628 (2008).

[8] ALTIN N., *Type-2 Fuzzy Logic Controller Based Maximum Power Point Tracking in Photovoltaic Systems.* Advances in Electrical and Computer Engineering 13: 65-70 (2013).

[9] Bouchafaa F., Hamzaoui I., Hadjammar A., *Fuzzy Logic Control for the tracking of maximum power point of a PV system.* Energy Procedia 6:152-159 (2011).

[10] Rezvani A., Gandomkar M., Izadbakhsh M., Vafaei S., *Optimal power tracker for photovoltaic system using ann-ga.* International Journal of Current Life Sciences 4: 107-111 (2014).

[11] Rai A.K., Kaushika N.D., Singh B., Agarwal N., *Simulation model of ANN based maximum power point tracking controller for solar PV system.* Solar Energy Materials and Solar Cells 95(2): 773-778 (2011).

[12] Cernazanu C., *Training Neural Networks Using Input Data Characteristics.* Advances in Electrical and Computer Engineering 8(2): 65-70 (2008).

[13] Fangrui L., Duan S., Liu F., Liu B., *A Variable Step Size INC MPPT Method for PV Systems.* IEEE Transaction on Industrial Electronics 55(7): 2622-2628 (2008).

[14] Esram T., Chapman P.L., *Comparison of photovoltaic array maximum power point tracking techniques.* IEEE Transactions on Energy Conversion 22: 439-449 (2007).

[15] Simoes M.G., Franceschetti N.N., *Fuzzy Optimisation Based Control of a Solar Array System.* Electric Power Applications 146(5): 552-558 (1999).

[16] Lee S., Kim J., Cha H., *Design and Implementation of Photovoltaic Power Conditioning System using a Current-based Maximum Power Point Tracking.* Journal of Electrical Engineering & Technology 5(4): 606-613 (2010).

[17] Hiyama T., Kouzuma S., Imakubo T., Ortmeyer T.H., *Evaluation of Neural Network Based Real Time Maximum Power Tracking Controller Far PV System*, IEEE Transaction On Energy Conversion 10(3): 543-548 (1995).

[18] Hiyama T., Kitabayashi K., *Neural Network Based Estimation of Maximum Power Generation from PV Module Using Environment Information.* IEEE Transaction on Energy Conversion 12(3): 241-247 (1997).

[19] Karatepe E., Boztepe M., Colak M., *Neural network based solar cell model.* Energy Conversion and Management 47(9-10): 1159-1178 (2006).

[20] Banu G., Suja S., *Fault location technique using GA-ANFIS for UHV line.* Archives of Electrical Engineering 63(2): 247-262 (2014).

[21] Rezvani A., Gandomkar M., Izadbakhsh M., Vafaei S., *Investigation of ANN-GA and modified perturb and observe MPPT techniques for photovoltaic system in the grid connected mode.* Indian Journal of Science and Technology 8(1): 87-95 (2015).

[22] Ramaprabha R., Gothandaraman V., Kanimozhi K., Divya R., Mathur B.L., *Maximum power point tracking using GA-optimized artificial neural network for Solar PV system.* [In:] IEEE 2011 Electrical Energy Systems (ICEES), Newport Beach, Calif, USA: IEEE, pp. 264-268 (2011).

[23] Vincheh M.R, Kargar A, GH.A., *A Hybrid Control Method for Maximum Power Point Tracking (MPPT) in Photovoltaic Systems.* Arabian Journal for Science and Engineering 39(6): 4715-4725 (2014).

[24] Izadbakhsh M., Gandomkar M., Rezvani A., Vafaei S., *Comparison of FLC-GA-PI Methods to Smooth the Output Power of Wind Turbine in the Grid Connected Mode.* SOP Transactions on Power Transmission and Smart Grid 1(1):44-59 (2014).
[25] Gasbaoui B., Abdelkader C.H., Adellah L., *Multi-input multi-output fuzzy logic controller for utility electric vehicle.* Archives of Electrical Engineering 60(3): 239-256 (2011).
[26] Yuan L.K., Chen Y., Chang Y., *MPPT Battery Charger for Stand-Alone Wind Power System*. IEEE Transaction on Industrial Electronics 26:1631-1638 (2011).
[27] Izadbakhsh M., Gandomkar M., Rezvani A., Vafaei S., *Dynamic Responses Improvement of Grid Connected WPGS using FLC in High Wind Speeds.* International Journal of Soft Computing, Mathematics and Control (IJSCMC) 3(4): 33-49 (2014).
[28] Lingfeng X., Xiyun Y., Xinran L., Daping X., *Based on adaptive fuzzy sliding mode controller.* [In:] IEEE 2008 in Intelligent Control and Automation WCICA 7th World Congress on china: IEEE, pp. 2970-2975 (2008).
[29] Amendola C.A.M., Gonzaga D.P., *Fuzzy-Logic Control System of a Variable-Speed Variable-Pitch Wind-Turbine and a Double-Fed Induction Generator.* [In:] IEEE 2007 Intelligent Systems Design and Applications, Seventh International Conference, Brazil: IEEE. pp. 252-257 (2007).
[30] Senjyu T., Sakamoto R., Urasaki N., Funabashi T., Sekine H., *Output power leveling of wind farm using pitch angle control with fuzzy neural network.* [In:] IEEE Power Engineering Society General Meeting, Japan: IEE, pp. 1- 8 (2006).
[31] Van T.L., Lee D.CH., *Output power smoothening of variable – speed wind turbine systems by pitch angle control.* [In:] IEEE 2012 Conference on Power & Energy, Ho Chi Minh City, China: IEEE, pp. 166-171 (2012).
[32] Das D., Esmaili R., Xu L., Nichols D., *An Optimal Design of a Grid Connected Hybrid Wind/Photovoltaic/Fuel Cell System for Distributed Energy Production*, 31st Annual Conference of IEEE Industrial Electronics, USA, pp. 2499-2504 (2005).
[33] Ahmed N.A., Miyatake M., Al-Othman A.K., *Power Fluctuations Suppression of Stand-Alone Hybrid Generation Combining Solar Photovoltaic/Wind Turbine and Fuel Cell Systems.* Energy Conversion and Management 49(10): 2711-2719 (2008).
[34] Balasubramanian G., Singaravelu S., *Fuzzy Controller for Stand Alone Hybrid PV-Wind Generation Systems*, International Journal of Soft Computing and Engineering (IJSCE) 2: 314-320 (2013).
[35] Esmaeili S., Shafiee S., *Simulation of Dynamic Response of Small Wind-Photovoltaic-Fuel Cell Hybrid Energy System*, Smart Grid and Renewable Energy 3:194-302 (2012).
[36] Cajethan N., Uchenna U.C., Theophilus M., *Wind-Solar Hybrid Power System for Rural Applications in the South Eastern States of Nigeria.* J. Electrical Systems 8: 304-316 (2012).
[37] Yang J, Honavar V. *Feature subset selection using a genetic algorithm.* IEEE Intelligent Systems, 13: 44-49 (1998).
[38] Arifujjaman Md., Modeling, *Simulation and Control of Grid Connected Permanent Magnet Generator (PMG)-based Small Wind Energy Conversion System*, In: IEEE Electrical Power & Energy Conference; Halifax, NS Canada: IEEE., pp. 1-6 (2010).
[39] Rosyadi M., Muyeen S.M., Takahashi R., Tamura J., *Transient stability enhancement of variable speed permanent magnet wind generator using adaptive pi-fuzzy controller.* [In:] IEEE PowerTech. Conference, Trondheim, Norway: IEEE. pp. 1-6 (2011).
[40] Blaabjerg F., Teodorescu R., Liserre M., Timbus A.V., *Overview of Control and Grid Synchronization for Distributed Power Generation Systems.* IEEE Transactions on Industrial Electronics 53(5): 1398-1409 (2006).
[41] Izadbakhsh M., Rezvani A., Gandomkar M., *Improvement of microgrid dynamic performance under fault circumstances using ANFIS for fast varying solar radiation and fuzzy logic controller for wind system.* Archives of Electrical Engineering 63(4): 551-578 (2014).